IAA-AAS-DyCoSS2 14-13-01

MHD REACTION WHEEL FOR SPACECRAFT ATTITUDE CONTROL: CONFIGURATION AND LUMPED PARAMETER MODEL

A. Salvati[*], **F. Curti**[†]

A novel actuator for spacecraft attitude control with liquid flywheel is presented. The main characteristic of this new concept of a reaction wheel is that a conductive liquid rather than a solid mass is accelerated to change the angular momentum of the equipment and, as a consequence, to provide the torque to the spacecraft. The conductive liquid inside an annulus with rectangular cross section is accelerated using the Lorentz force originates from the interaction between an electric current flowing through the fluid and a magnetic field. This paper proposes two suitable configurations of the device and a lumped parameter model based on Magneto-Fluid Dynamics set of equations under the hypothesis of low Magnetic Reynolds. The lumped parameter model is addressed to one of the two configurations considered more suitable for space application.

INTRODUCTION

The ability to control spacecraft attitude is a key component of all missions where space and power is at a premium as with smaller satellites especially if keeping a high value of the reliability. Also, future Earth observation missions as well as astronomical observation missions require satellites which are more agile (moving their direction of pointing) and with higher pointing stability (so as to provide better resolution images) over the higher lifetime possible.
A number of techniques have been developed and refined to underpin attitude control and re-pointing but basically since the beginning of the space exploration era all techniques used for high performance attitude control exploit the use of reaction and (in some cases) momentum wheels.
The technology improvement during this time allowed reaction wheels to improve their performances in terms of control resolution and reliability and efficiency of the electronic part but there are some drawbacks related to standard reaction wheel design that were not improved over time. In particular we can mention some of the more important like:

- Standard reaction wheels use moving mechanical parts which reduce the overall reliability of the equipment and increase its overall complexity.
- Jitter and other unbalances associated with moving masses and classical electric motors lead to unwanted high frequency disturbances on the satellite itself which could be critical for demanding high resolution observation missions.

[*]PhD Candidate. "Sapienza" University of Rome, Italy, DIAEE Department, ARCA lab.
E-mail: alessandro.salvati@uniroma1.it
[†]Associate Professor. "Sapienza" University of Rome, Italy, DIAEE Department, ARCA lab.
E-mail: fabio.curti@uniroma1.it

In the last years some articles have been published regarding the possibilities to use active fluid loops as actuator for spacecraft attitude control, References [1] [2]. This kind of actuators uses an hydraulic pump to accelerate a low viscosity liquid inside a torus with circular cross section. These devices have the advantage to reduce the mechanical unbalances typical of classical reaction wheels with solid flywheel but they do not increase the reliability of the actuator because of the presence of a spinning electric engine in the hydraulic pump.
The electric engine can be removed using a conductive liquid and a conductive magneto-hydrodynamic pump in order to use no moving component to accelerate the liquid, References [3] [4]

CONFIGURATIONS OF THE DEVICE

The main feature of this new concept of reaction wheel is that a conductive fluid rather than a solid mass is accelerated to change the angular momentum and to provide a controlling torque to the spacecraft. The Lorentz force is used to accelerate the conductive liquid. This driving force originates from the interaction between a magnetic field and an electric current flowing through the fluid. This implies that no mechanical moving parts are needed to speed up the conductive fluid.
The liquid is placed in an annulus with a rectangular cross section and it rotates along the azimuthal direction. The Lorentz force acts in the direction in which the conductive fluid is free to flow; two different configurations have been evaluated, Figure 1:

- the first configuration takes into account an electric current along the radial direction r and a magnetic field along the axial direction z.
- the second configuration switches the first configuration considering an electric current along the z direction and a magnetic field along the r direction.

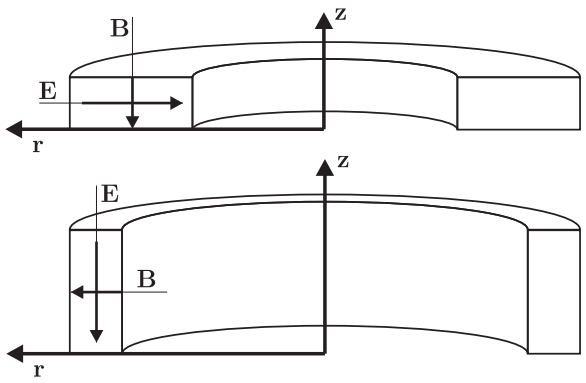

Figure 1: First (top) and second configuration (bottom) for electric field E and magnetic field B

The two configurations provide a force in the requested direction.The advantage to use one of two configurations has been evaluated on the base of the maximization of the dimensionless moment of inertia.
We start pointing out that in both the configurations the dimension parallel to the magnetic field is constrained in order to have an homogeneous magnetic field in the air gap of the magnetic circuit. It means that the height of the device in the first configuration and the radial length of the cross section

in the second one can not be greater than a certain value.
The dimensionless moment of inertia $\tilde{I}_z$ for an hollow cylinder can be expressed as:

$$I_z = \frac{m\left(r_e^2 + r_i^2\right)}{2} \qquad \tilde{I}_z = \frac{I_z}{m r_e^2} = \frac{1+\beta^2}{2} \tag{1}$$

where r_e is the outer radius of the hollow cylinder, r_i is the inner radius of the hollow cylnder, β is the ratio r_i/r_e and m is the mass of the liquid. We can see that $\tilde{I}_z$ is independent from the height of the cylinder.

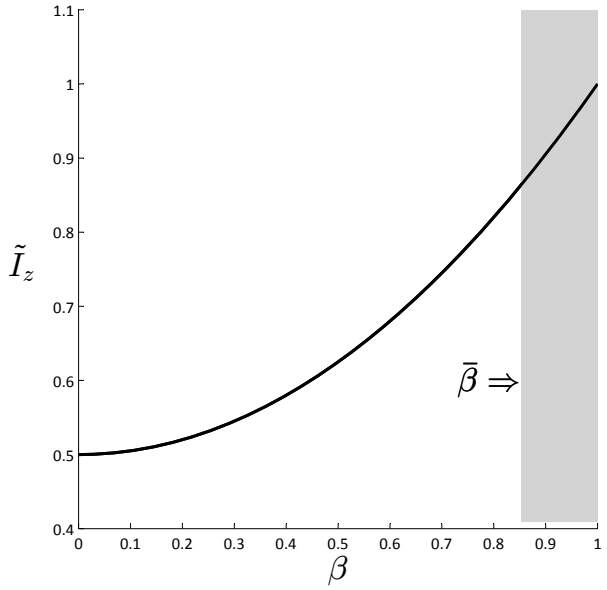

Figure 2: Dimensionless Moment of Inertia to Mass ratio

If we consider the mimimum inner radius of the second configuration to be a fraction $\bar{\beta}$ of the outer radius we can see in Figure 2 that the grey zone is the characteristic $\tilde{I}_z$ for the second configuration while the complete plot can be referred to the first configuration. We notice that the dimensionless moment of inertia to mass ratio is in general greater for the second configuration. The first configuration has the same $\tilde{I}_z$ of the second one only in the grey zone where anyway it has low absolut moment of inertia due to the limitation on its height.

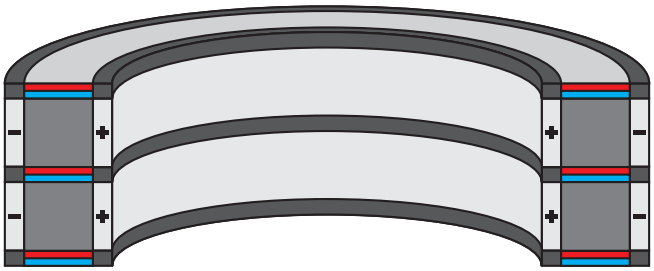

Figure 3: MHD Fluid Loop - 1^{st} Configuration

We could think to stack several annuli according to the first configuration in order to obtain the desired moment of inertia while optimizing the dimensionless moment of inertia, Figure 3, as already studied in Reference[4]. This approach, anyway, would increase the contact surface between the liquid and cavity, and then the viscous shear, more than how it would increase choosing the second configuration.
We can conclude that the second configuration, characterized by a radial magnetic field and an axial electric field, maximizes the dimensionless moment of inertia while optimizing the contact surface of the conductive liquid. It represents a more easily scalable configuration in which the required moment of inertia of the liquid flywheel can be met just varying the height of device.
The device, according to the selected configuration, has electric plates on the top and on the bottom sides and two concentric cylindrical magnets generating a radial magnetic field. The conductive fluid is placed in the air gap of the hollow cylinder, Figure (4). The spin direction of the liquid can be switched by changing the direction of the electric field between the two plates.

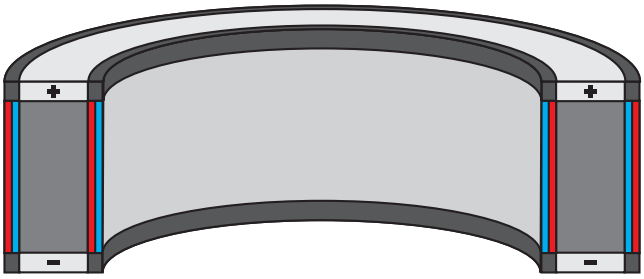

Figure 4: MHD Fluid Loop - 2^{nd} Configuration

MHD COMPLETE SET OF EQUATIONS - LOW MAGNETIC REYNOLDS

The physics of the Magneto-Hydro-Dynamics (MHD) phenomena is generally described by a set of equations that takes into account the mutual interactions among the velocity, the electric field and the magnetic field. The complete set of equations can be simplified in the study. We assume that the velocity and the electric field do not affect the magnetic field. This assumption is usually true when the Magnetic Reynolds number R_m is much lower than one. The Magnetic Reynolds number is defined as $R_m = \mu_m \sigma U_0 L$ where μ_m and σ are the magnetic permeability and the electric conductivity of the liquid, U_0 is the mean velocity of the fluid and L is the thickness of the air gap. In the study we will consider conductive and paramagnetic liquids so that $\mu_m \sigma \sim 1 s/m^2$, $L \sim 0.01m$ with a viscosity that gives values of U between $0.01m/s$ and $1m/s$. This gives $R_m \sim 10^{-4} \div 10^{-2}$

for which the magnetic field can be considered steady and equal to the applied magnetic field, Reference[5]. The complete set of equations for a laminar flow and Low Magnetic Reynolds is given as follows:

$$\nabla \cdot \mathbf{B} = 0 \tag{2}$$

$$\nabla \cdot \mathbf{J} = 0 \tag{3}$$

$$J = \sigma(\mathbf{E} + \mathbf{U} \times \mathbf{B}) \tag{4}$$

$$\nabla \times \mathbf{E} = 0 \tag{5}$$

$$\rho \frac{\partial \mathbf{U}}{\partial t} = \nu \rho \Delta \mathbf{U} + \mathbf{J} \times \mathbf{B} \tag{6}$$

Eq.(2) states that the conservation of magnetic flux density can be solved by imposing the boundary condition on one of the vertical boundaries of the cross section. Eq.(3) and Eq.(4) describe respectively the conservation of the electric current and the coupling between the induced electric field and the current distribution. Eq.(5) states the irrotationality condition of the electric field valid for phenomena with stationary magnetic field and Eq.(6) is the Navier-Stokes equation for laminar flows.

MONODIMENSIONAL SOLUTION UNDER THE HYPOTHESIS OF LOW-MAGNETIC REYNOLDS

For convenience we proceed writing the whole set of equation in dimensionless variables. We obtain:

$$\nabla' \cdot \mathbf{b} = 0 \tag{7}$$

$$\nabla' \cdot \mathbf{j} = 0 \tag{8}$$

$$\mathbf{j} = \mathbf{e} + \mathbf{u} \times \mathbf{b} \tag{9}$$

$$\nabla' \times \mathbf{e} = 0 \tag{10}$$

$$\frac{\partial \mathbf{u}}{\partial \tau} = \frac{1}{Re} \Delta' \mathbf{u} + \frac{Ha^2}{Re} \mathbf{j} \times \mathbf{b} \tag{11}$$

$$s = \frac{r}{r_e} \tag{12}$$

$$\nabla' \cdot \mathbf{u} = 0 \tag{13}$$

in which the following substitutions have been done:

$$\mathbf{u} = \frac{\mathbf{U}}{U_0} \tag{14}$$

$$\mathbf{b} = \frac{\mathbf{B}}{B_0} \tag{15}$$

$$\mathbf{e} = \frac{\mathbf{E}}{B_0 \, U_0} \tag{16}$$

$$\mathbf{j} = \frac{\mathbf{J}}{\sigma\, B_0\, U_0} \tag{17}$$

$$\tau = \frac{t\, U_0}{L} \tag{18}$$

$$\nabla' = L\, \nabla \tag{19}$$

The coefficients in Eq.(11) are the Hartmann Number, Ha defined as $B_0 L\sqrt{\sigma/\mu}$ and the Reynolds number, Re, defined as $\rho L U_0/\mu$. In Eqs.(14)-(19) U_0 has the meaning of average velocity of the fluid, B_0 is the magnetic field density at the outer radius and r_e is the outer radius of the liquid flywheel.

The main simplifying assumption adopted is to consider infinite the length of the annulus along the axis of symmetry. It implies the neglection of the boundary effects next to the two electric armatures and it implies moreover that all the derivative along z are considered neglectible. The superimposed magnetic field is assumed to be dependent just from the radial coordinate. This assumption together with the uniformity of the imposed electric field $\mathbf{e}$ makes the problem axially symmetric, i.e. all the derivative with respect of the azimuthal direction can be neglected. We start by analyzing the continuity equations of the magnetic flux density $\mathbf{b}$, current density $\mathbf{j}$ and velocity $\mathbf{u}$.

It is possible to simplify the continuity equations for the dimensionless magnetic flux density $\mathbf{b}$, Eq.(7), the dimensionless electric current density $\mathbf{j}$, Eq.(8), and the dimensionless velocity of the fluid $\mathbf{u}$, Eq.(13). Introducing the expression of the divergence in cylindrical coordinates and simplifying we obtain:

$$\nabla\mathbf{b} = \frac{1}{s}\frac{\partial}{\partial s}(sb_r) + \frac{1}{s}\frac{\partial b_\theta}{\partial \theta} + \frac{\partial b_z}{\partial z} = \frac{\partial}{\partial s}(sb_r) = 0 \tag{20}$$

$$\nabla\mathbf{j} = \frac{1}{s}\frac{\partial}{\partial s}(sj_r) + \frac{1}{s}\frac{\partial j_\theta}{\partial \theta} + \frac{\partial j_z}{\partial z} = \frac{\partial}{\partial s}(sj_r) = 0 \tag{21}$$

$$\nabla\mathbf{u} = \frac{1}{s}\frac{\partial}{\partial s}(su_r) + \frac{1}{s}\frac{\partial u_\theta}{\partial \theta} + \frac{\partial u_z}{\partial z} = \frac{\partial}{\partial s}(su_r) = 0 \tag{22}$$

with the following boundary condition at the outer radius:

$$\begin{aligned} & & b_r(s_0,\tau) = 1 \\ s_0 = 1 \quad & & j_r(s_0,\tau) = 0 \\ & & u_r(s_0,\tau) = 0 \end{aligned} \tag{23}$$

Solving Eqs.(20)-(22) using Eqs.(23) we obtain:

$$b_r(s,\tau) = \frac{1}{s} \tag{24}$$

$$j_r(s,\tau) = 0 \tag{25}$$

$$u_r(s,\tau) = 0 \tag{26}$$

The axial component of the dimensionless velocity, u_z, can be studied taking into account the Eq.(11) along z:

$$\frac{\partial u_z}{\partial \tau} = \frac{\lambda^2}{Re}\left[\frac{1}{s}\frac{\partial}{\partial s}\left(s\frac{\partial u_z}{\partial s}\right)\right] + \frac{Ha^2}{Re} j_\theta b_r \tag{27}$$

Using the hypothesis of axial-symmetry it is possible to say that the component along θ of the current density j_θ is null both because of the radial distribution of the magnetic field and because of the uniformity of the electric field applied. This result leads the Eq. (27) to be a homogeneous PDE with homogeneous boundary condition due to the no-slip condition applied at the boundaries to the velocity field. Furthermore and without lack of generality we can impose that the fluid is at rest at the initial time $\tau = 0$. This problem gives a null solution over the time for the u_z:

$$u_z(s, \tau) = 0 \tag{28}$$

Writing the Eq.(9) along the three directions of cylindrical reference frame and being the dimensionless velocity purely azimuthal and the magnetic flux density purely radial we have:

$$\begin{aligned} e_r &= j_r - u_\theta b_z + u_z b\theta = 0 \\ e_\theta &= j_\theta - u_z b_r + u_r bz = 0 \\ e_z &= j_z - u_r b_\theta + u_\theta b_r = j_z + u_\theta b_r \end{aligned} \tag{29}$$

The Eq.(10) that describes the irrotationality of the applied electric field is solved taking into account the hypothesis that the component of the electric field along the z direction is uniform. In other words if we consider each armature equipotential we can see that the electric field along the z direction does not vary along the radial and azimuthal directions.
Finally we obtain the complete set of equation for magneto-fluid problems under the hypothesis of Low-Magnetic Reynolds reduced to the the following system of three equations:

$$b_r = \frac{1}{s} \tag{30}$$

$$j_z = e_z - u_\theta b_r \tag{31}$$

$$\frac{\partial u_\theta}{\partial \tau} = \frac{\lambda^2}{Re}\frac{\partial}{\partial s}\left[\frac{1}{s}\frac{\partial}{\partial s}\left(s u_\theta\right)\right] + \frac{Ha^2}{Re} j_z b_r \tag{32}$$

in which Eq.(30) is already solved and just Eqs.(31)-(32) are coupled. Starting from the hypothesis of Low-Magnetic Reynolds the same equations as in Reference[6] has been found and we can use the same solution proposed in the paper.
Writing the Eq.(32) with the same symbology as in Reference[6] and introducing the Eq.(31) we have:

$$\frac{\partial u_\theta}{\partial \tau} = C_1\left[\frac{\partial^2 u_\theta}{\partial s^2} + \frac{1}{s}\frac{\partial u_\theta}{\partial s} - \frac{m^2 u_\theta}{s^2}\right] + C_2\frac{e_z}{s} \tag{33}$$

where:

$$\begin{aligned} C_1 &= \lambda^2/Re \qquad & C_2 &= Ha^2/Re \\ \lambda &= L/R \qquad & m^2 &= 1 + Ha^2/\lambda^2 \end{aligned} \tag{34}$$

In Reference[6] two solutions are given: one steady-state solution and one time-dependent solution. Looking at the purpose to obtain a lumped parameter model we show more interest in the stationary solution in which the influence of the electric current and the shape of velocity profile can be easily uncoupled instead of considering the transient solution that gives a time dependent solution but by which is not possible to derive a lumped parameter model.
The steady-state solutions for the velocity and the angular velocity is:

$$U_\theta(r) = \frac{E_z}{B_0}\left[A_1 r - A_2 r^m - A_3 \frac{1}{r^m}\right] \tag{35}$$

$$\omega_z(r) = \frac{U_\theta(r)}{r} = \frac{E_z}{B_0}\left[A_1 - A_2 r^{m-1} - A_3 \frac{1}{r^{m+1}}\right] \tag{36}$$

where:

$$A_1 = \frac{1}{R} \quad A_2 = \frac{1-\beta^{m+1}}{(1-\beta^{2m})R^m} \quad A_3 = \frac{\beta^{m+1}\left(1-\beta^{m-1}\right)R^m}{1-\beta^{2m}} \tag{37}$$

and

$$\beta = 1 - \lambda \tag{38}$$

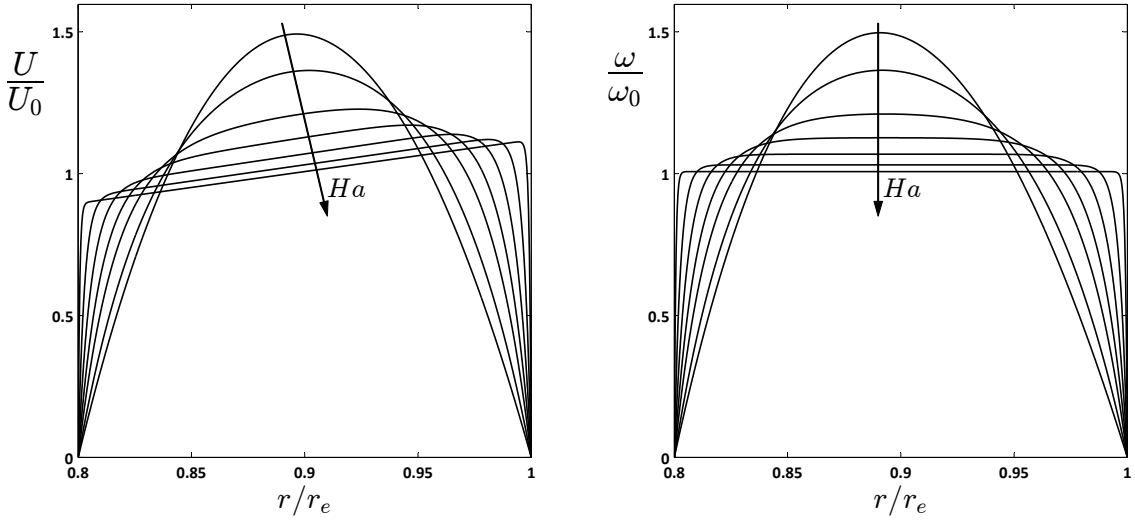

Figure 5: Analytical solutions for dimensionless linear and angular velocities at different Hartmann Number Ha.

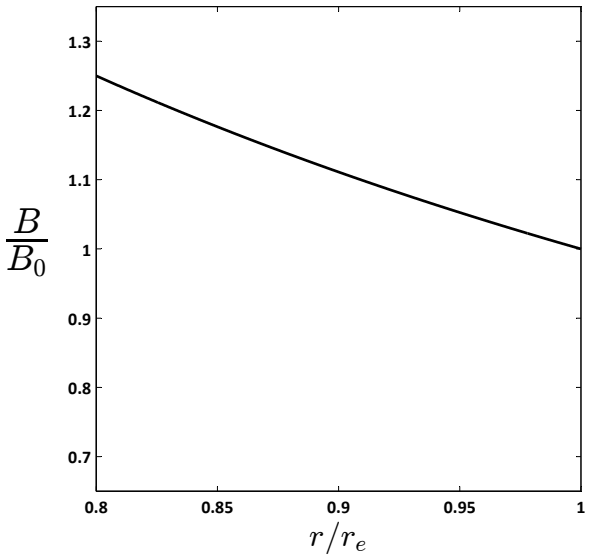

Figure 6: Magnetic Field Density $\mathbf{B}$ normalized with respect of the Magnetic Field Density B_0 at the outer radius.

The shape of the dimensional magnetic field B can be obtained from the Eqs.(15)-(30):

$$\mathbf{B}(r) = \frac{B_0 r_e}{r} \tag{39}$$

where B_0 is the value of the magnetic field at $r = r_e$. The solution is expressed in dimensional quantities. The coefficients m and β in Eq.(35) are function of the physical property of the conductive fluid and of the dimension along the direction r of the cavity containing the fluid. The solution can be considered expressed in the reference frame of the spacecraft with the meaning of relative velocity between the liquid and the case.

LUMPED PARAMETER DYNAMIC MODEL

In order to derive the dynamic part of the Lumped Parameter model we consider the Navier Stokes equation through an integral balance of moments along the z direction.

$$\int_V \rho r \hat{\mathbf{r}} \times \frac{\partial U_\theta}{\partial t} \hat{\boldsymbol{\theta}} dV = \int_V r \hat{\mathbf{r}} \times [J_z B(r)] \hat{\boldsymbol{\theta}} dV + \int_S \mu r \hat{\mathbf{r}} \times \left[r \frac{\partial}{\partial r} \left(\frac{U_\theta}{r} \right) \right] \hat{\boldsymbol{\theta}} dS \tag{40}$$

The stationary solution derived in the previous section can be used to obtain quantitative evaluation of the viscous shear at the boundaries together with an equivalent moment of inertia of the spinning liquid and the back electromotive force generated by the spinning liquid inside the superimposed magnetic field. Being the analytical solution monodimesional we expect the model to underestimate the viscous shear and overestimate the BEMF and the equivalent moment of inertia.
Anyway the quantitative estimation of the proposed model is as closer to the axis-symmetrical 2-dimensional solution as the height of the cross section become big compared to its dimension along the direction r. This hypothesis can be relaxed for high Hartmann number where the characteristic

length of interaction between the liquid and the boundary became very tiny and the velocity profile of the liquid show rigid body-like behaviour. To compute the viscous shear moment, we consider the last term of right side of Eq.(40) and we obtain for one of the boundaries:

$$M_{vis} = \int_S \mu r^2 \frac{d}{dr}\left(\frac{U_\theta(r)}{r}\right)\hat{\mathbf{z}}dS = \mu S r^2 \frac{d\omega_z(r)}{dr} \tag{41}$$

Considering both the boundaries at r_i and r_e we have:

$$M_{vis} = K_{vis}\omega_w \tag{42}$$

where:

$$K_{vis} = \frac{\mu S}{\omega_0}\left(r_i^2 \frac{d\omega_z(r)}{dr}\bigg|_{r=r_i} + r_e^2 \frac{d\omega_z(r)}{dr}\bigg|_{r=r_e}\right) \tag{43}$$

The torque generates by the Lorentz Force can be derived from the first term of the right side of the (40). Introducing the shape of the radial magnetic field we have:

$$M_{Lor} = \int_V \mathbf{r} \times \hat{\theta}\left(J_z B_r\right) dV = B_0 r_i h I = K_I I \tag{44}$$

where:

$$K_I = B_0 r_i h \tag{45}$$

The term of the left side of the (40) represents the resulting torque acting on the conductive fluid, i.e. the time derivative of the angular moment. In order to have this term function of the only time derivative of the average velocity of the fluid we start considering the angular moment in the reference frame of the spacecraft:

$$\Gamma = \int_V \rho r^2 \omega_z(r)\,\hat{\mathbf{z}}dV = \omega_w c_\omega I_z \hat{\mathbf{z}} \tag{46}$$

where:

$$c_\omega = \frac{2\pi h\rho \int_{r_i}^{r_e} r^3 \omega_z(r)\,dr}{\omega_0 I_z} \tag{47}$$

and I_z is the moment of inertia of a rigid hollow cylinder with the same dimensions of the cavity containing the liquid. In this way the time-derivative of the angular moment can be considered as:

$$\dot{\Gamma} = \dot{\omega}_w c_\omega I_z \tag{48}$$

due to invariance with respect of the time of the coefficient c_ω.

LUMPED PARAMETER ELECTRIC MODEL

A formula for the lumped parameter electric model of the proposed MHD reaction wheel can be obtained by integrating over the volume the microscopic Ohm's Law for moving conductor and introducing the relative velocity between the liquid and the magnetic field considered stiffly linked to the boundaries:

$$\int_V E_z dz dS = \int_V \frac{J_z}{\sigma} dz dS + \int_V r w_z(r) B_r dz dS \tag{49}$$

Considering the electric potential ϕ uniform over the surface and applying the conservation of the electric current we obtain:

$$\Delta\phi = I\frac{h}{\sigma S} + \frac{\int_V r w_z(r) B_r dz dS}{S} \tag{50}$$

where the coefficient of the electric current is the equivalent electric resistance of the conductive liquid:

$$R_{eq} = \frac{h}{\sigma S} \tag{51}$$

The second term on the right side of the (49) is the induced tension that can be written as:

$$\Delta\phi_{ind} = K_V \omega_w \tag{52}$$

where:

$$K_V = 2\pi B_0 r_i h \frac{\int_{r_i}^{r_e} r w_z(r)\, dr}{\omega_0 S} \tag{53}$$

LUMPED PARAMETER MODEL

Assembling the results found in the previous sections, the Lumped Parameter 1-dof model of the spacecraft-MHD reaction wheel system has been obtained:

$$\begin{cases} I_s \ddot{\theta}_s = -M + D \\ M = I_z\left(\ddot{\theta}_s + c_\omega \dot{\omega}_w\right) = -K_{vis}\omega_w + K_I I \\ \Delta\phi = R_{eq} I + K_V \omega_w \end{cases} \tag{54}$$

In the model the angular velocity of the fluid has the meaning of relative angular velocity between the fluid and the case of the reaction wheel.
The model is similar to the model of the classic reaction wheel with an extra-term taking into account the viscous torque, proportional to the relative angular velocity ω_w. This term leads to a slight different behaviour of the Torque-Current characteristic: while, for the classical reaction wheel, the torque provided is constant when the electric current fed to the device is constant, here, the torque is constant if the electric current varies linearly over the time. This results can be proved

by reducing the lumped parameter model to the only wheel, considering the case of the MHD reaction wheel not able to rotate.
From Eq.(54), removing the coupling with the spacecraft dynamics, we obtain:

$$\begin{cases} I_z c_\omega \dot{\omega}_w + K_{vis}\omega_w = K_I I \\ \Delta\phi = K_V \omega_w + R_{eq} I \end{cases} \tag{55}$$

Considering a generic current drive for the device and homogeneous initial conditions, we obtain from the first of Eq. (55) the following solution:

$$\omega_w(t) = e^{-\frac{K_{vis}}{I_z c_\omega} t} \int_0^t \frac{K_I}{I_z c_\omega} \, I(\tau) \, e^{\frac{K_{vis}}{I_z c_\omega} \tau} \, d\tau \tag{56}$$

If we now apply a linear law to the electric current:

$$I(t) = at \tag{57}$$

the solution (56) becomes:

$$\omega_w(t) = \frac{K_I}{K_{vis}} at - \frac{I_z c_\omega K_I a}{K_{vis}^2} \left[1 - e^{-\frac{K_{vis} t}{I_z c_\omega}} \right] \tag{58}$$

and the torque provided is:

$$T(t) = I_z c_\omega \dot{\omega}_w(t) = I_z c_\omega \frac{K_I}{K_{vis}} a \left[1 - e^{-\frac{K_{vis} t}{I_z c_\omega}} \right] \tag{59}$$

that after a transient becomes constant for a linear electric current:

$$T \to I_z c_\omega \, a \frac{K_I}{K_{vis}} \tag{60}$$

Taking into account a constant electric current I:

$$I(t) = I \tag{61}$$

we find that the angular momentum Γ is:

$$\Gamma(t) = I_z c_\omega \omega_w(t) = I_z c_\omega \frac{K_I}{K_{vis}} I \left[1 - e^{-\frac{K_{vis} t}{I_z c_\omega}} \right] \tag{62}$$

and its regime value is:

$$\Gamma \to I_z c_\omega \frac{K_I}{K_{vis}} I \tag{63}$$

The Eqs.(59)(62) show that the reaction of the system to a current drive has a characteristic time:

$$\tau_c = \frac{I_z c_\omega}{K_{vis}} \tag{64}$$

The power consumption in the stationary case for a constant electric current is:

$$P = \left(\frac{K_V K_I}{K_{vis}} + R_{eq} \right) I^2 \tag{65}$$

PERFORMANCES ANALYSIS.

Considering mercury as conductive fluid with the following physical properties:

$$\begin{aligned} \sigma_{Hg} &= 1.04 \cdot 10^6 \; S/m \\ \rho_{Hg} &= 1.36 \cdot 10^4 \; Kg/m^2 \\ \mu_{Hg} &= 1.50 \cdot 10^{-3} \; Pa/s \end{aligned} \tag{66}$$

the coefficients of the lumped parameter model together with the torque and the power consumption are presented in Figures(7)-(15). All the values plotted in the following figure, expect for c_ω that is dimensionless, are calculated for a torus with rectangular cross section whose height is equal to $h = 1cm$. The symbols on the y axys of Fig.(11), Fig.(12) and Fig.(15) have the following meaning:

$$\frac{\omega_w}{I} = \frac{\Gamma}{I_z \; c_\omega I} = \frac{K_I}{K_{vis}} \tag{67}$$

$$\tilde{T} = \frac{T}{ah} = \frac{1}{h} \left(I_z c_\omega \; \frac{K_I}{K_{vis}} \right) \tag{68}$$

$$\tilde{P} = \frac{P}{hI^2} = \frac{1}{h} \left(\frac{K_V K_I}{K_{vis}} + R_{eq} \right) \tag{69}$$

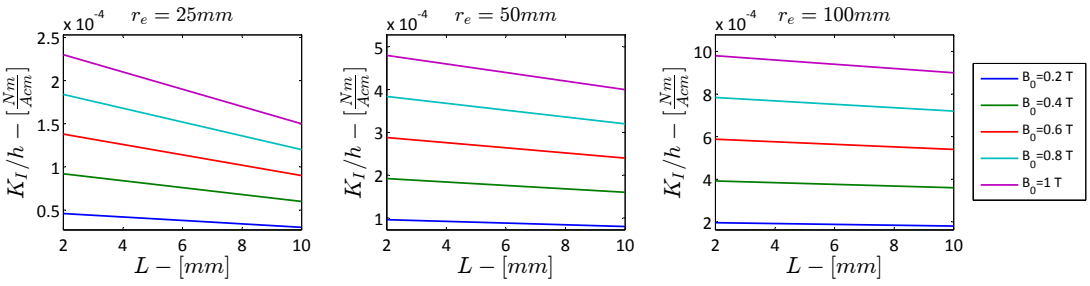

Figure 7: K_I function of L for $B_0 = 0.2 \div 1.0$ and 3 different outer radii $r_e = 25, 50, 100mm$. Liquid: Mercury (Hg).

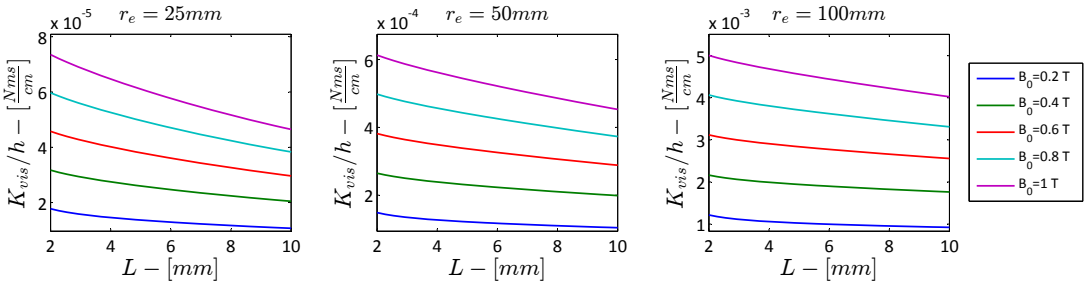

Figure 8: K_{vis} function of L for $B_0 = 0.2 \div 1.0$ and 3 different outer radii $r_e = 25, 50, 100mm$. Liquid: Mercury (Hg).

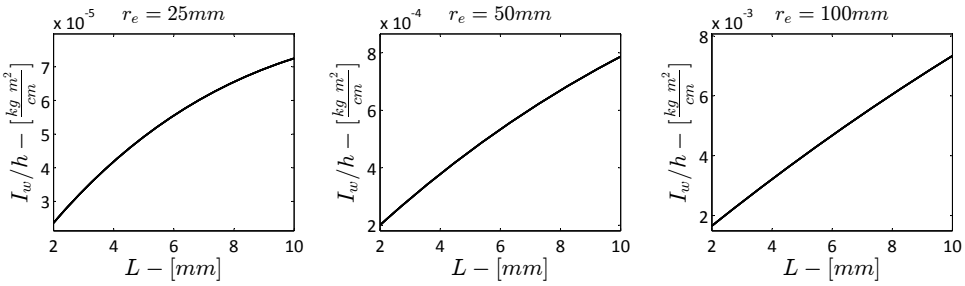

Figure 9: I_w function of L for 3 different outer radii $r_e = 25, 50, 100mm$. Liquid: Mercury (Hg).

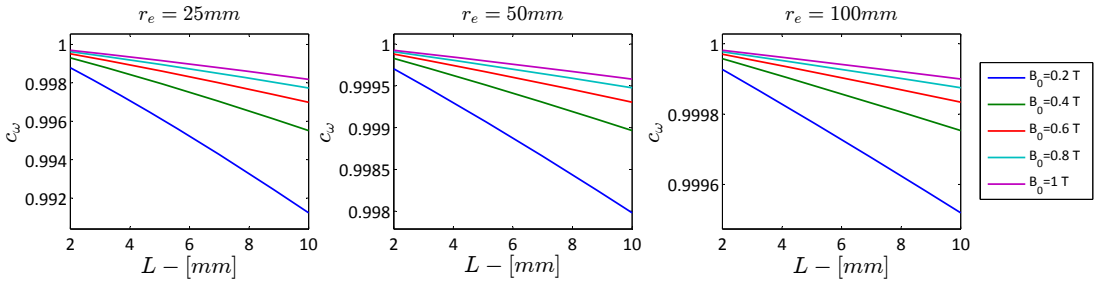

Figure 10: c_ω function of L for $B_0 = 0.2 \div 1.0$ and 3 different outer radii $r_e = 25, 50, 100mm$. Liquid: Mercury (Hg).

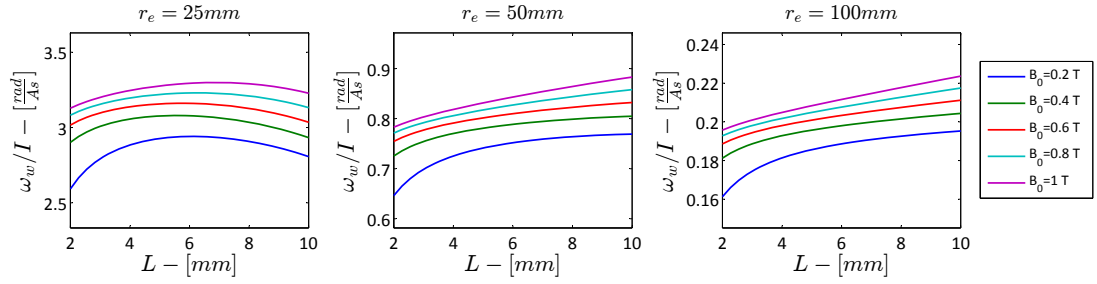

Figure 11: Current specific ω_w function of L for $B_0 = 0.2 \div 1.0$ and 3 different outer radii $r_e = 25, 50, 100mm$. Liquid: Mercury (Hg).

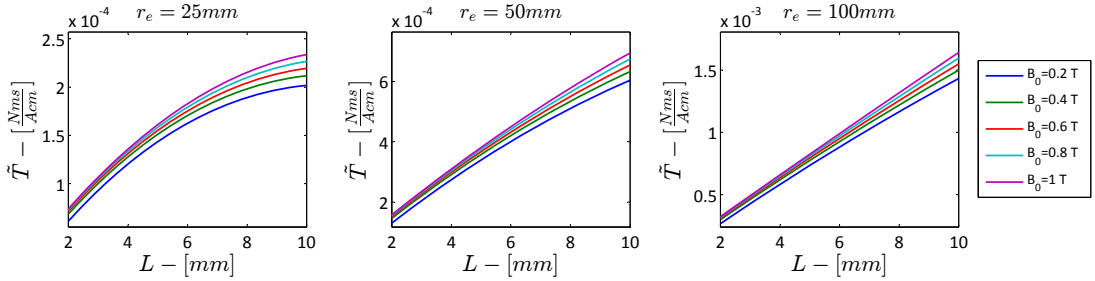

Figure 12: Torque function of L for $B_0 = 0.2 \div 1.0$ and 3 different outer radii $r_e = 25, 50, 100mm$. Liquid: Mercury (Hg).

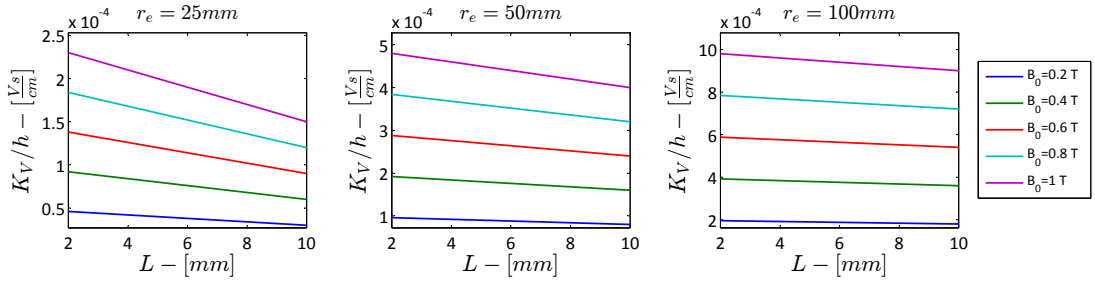

Figure 13: K_V function of L for $B_0 = 0.2 \div 1.0$ and 3 different outer radii $r_e = 25, 50, 100mm$. Liquid: Mercury (Hg).

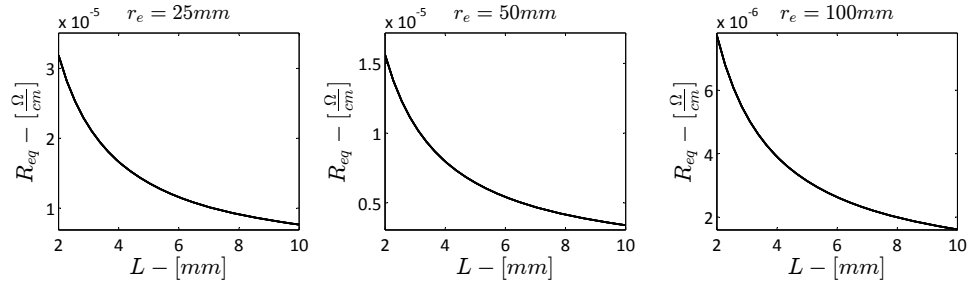

Figure 14: R_{eq} function of L for 3 different outer radii $r_e = 25, 50, 100mm$. Liquid: Mercury (Hg).

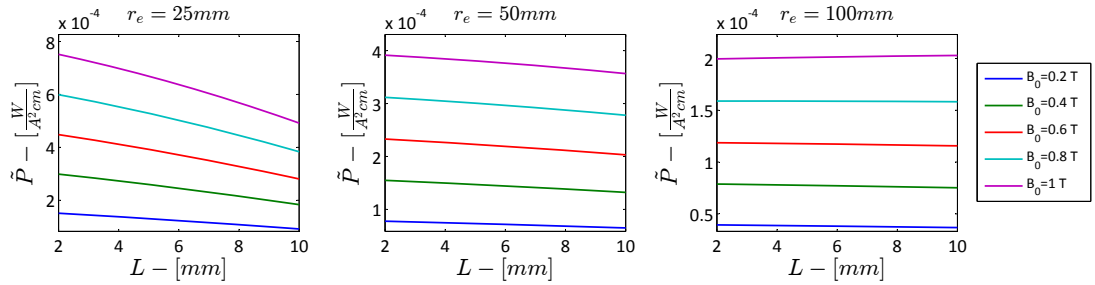

Figure 15: Power consumption function of L for $B_0 = 0.2 \div 1.0$ and 3 different outer radii $r_e = 25, 50, 100mm$. Liquid: Mercury (Hg).

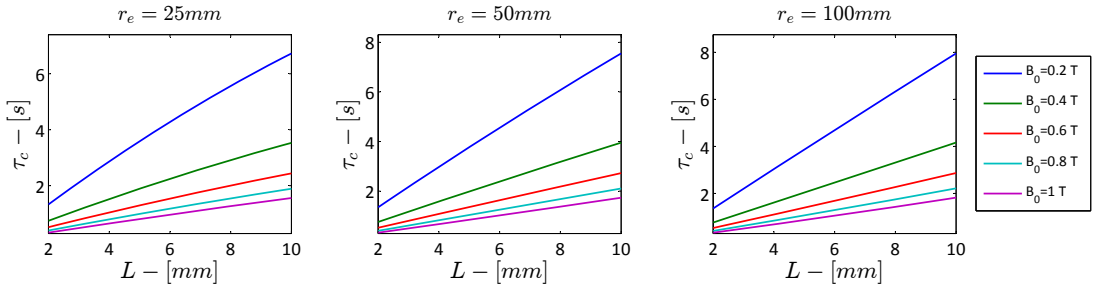

Figure 16: Characteristic time function of L for $\sigma = 10 \div 10^6\ S/m$ and 3 different outer radii $r_e = 25, 50, 100mm$. $B_0 = 1.0\ T$. $\rho = 1000\ Kg/m^3$.

From Figure(8) it is possible to see that the influence of the viscosity is not neglectable and it influences the overall performances of the device. The high value of the K_{vis} is proportional to the electrical conductivity of the fluid due to the coupling between the induced voltage and the velocity profile. The values of K_{vis} have been analyzed for different electrical conductivities of the liquid together with the power consumption $\tilde{P}$ and the generated torque $\tilde{T}$. The values are calculated for a liquid with density $\rho = 1000\ Kg/m^3$ and viscosity $\mu = 10^{-3}\ Pa\ s$; the magnetic field is set to $B_0 = 1\ T$.

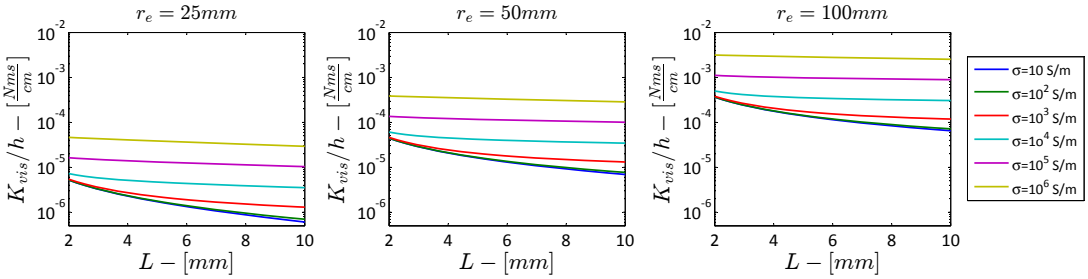

Figure 17: K_{vis} function of L for $\sigma = 10 \div 10^6\ S/m$ and 3 different outer radii $r_e = 25, 50, 100mm$. $B_0 = 1.0\ T$. $\rho = 1000\ Kg/m^3$.

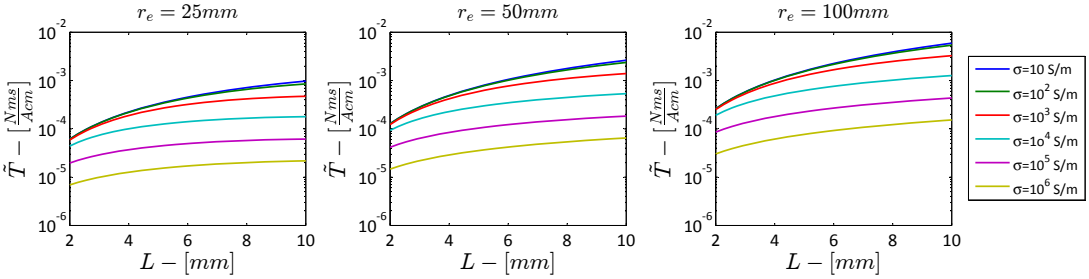

Figure 18: Torque function of L for $\sigma = 10 \div 10^6\ S/m$ and 3 different outer radii $r_e = 25, 50, 100mm$. $B_0 = 1.0\ T$. $\rho = 1000\ Kg/m^3$.

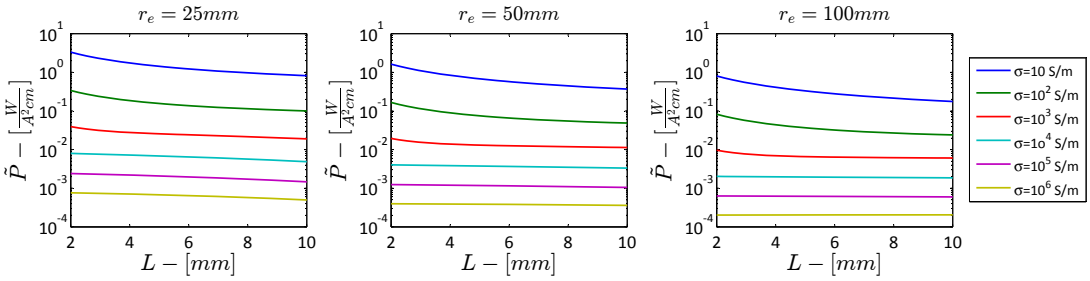

Figure 19: Power consumption function of L for $\sigma = 10 \div 10^6\ S/m$ and 3 different outer radii $r_e = 25, 50, 100mm$. $B_0 = 1.0\ T$. $\rho = 1000\ Kg/m^3$.

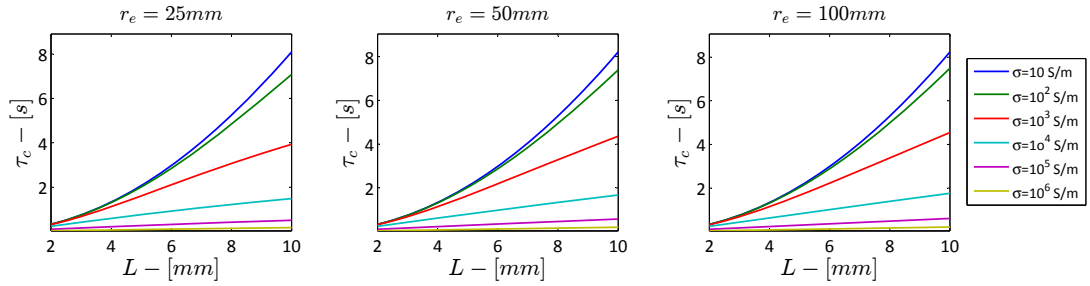

Figure 20: Characteristic time function of L for $\sigma = 10 \div 10^6\ S/m$ and 3 different outer radii $r_e = 25, 50, 100mm$. $B_0 = 1.0\ T$. $\rho = 1000\ Kg/m^3$.

From Figures(17) and (18) it is possible to see the improving in the performances for low conducting fluid. Due to the low coupling between the velocity and the magnetic field, the generated torque for a low conductive fluid become bigger of at about two orders of magnitude with respect of an high conductive fluid. As expected, the power consumption has an opposite trend but its maximum value is anyway around $1W$ if an electric current of $1A$ is applied, Figure(19).
For high conductive fluids the estimation of the parameters is expected to be quite accurate due to the fact that the length of the boundary layers on the upper and bottom walls scale as $\delta_{Sh} \sim 1/\sqrt{Ha}$ while the boundary layers on the lateral surfaces scale as $\delta_{Ha} \sim 1/Ha$, Reference [7] . For high Ha these two characteristic length can differ of one order of magnitude, then the error due to the neglection of the Shercliff layers, next to the armatures, is low.
On the other side the prediction of K_{vis} and the available torque could be regarded as not accurate for very low conductive fluid due to the reason that the Shercliff layers on the upper and bottom surface of the torus are in this case of the same order of magnitude of the Hartmann layers on the lateral walls of the torus. Anyway the density of an hypothetical low conductive fluid is expected to be low if compared with the density of a liquid metal. This implies that in order to have the same moment of inertia in both the cases of high and low conductive fluid, the height of the cross section will be bigger than the radial dimension of the cross section if the working fluid has low electric conductivity. This implies again that the viscous shear on the top and bottom boundaries could be neglectable with respect of the viscous shear acting on the lateral cylindrical surfaces of the device.

CONCLUSIONS

In this paper we propose a system configuration for an MHD reaction wheel. A stationary monodimensional analytical solution has been derived; it can be compared with the one found in Reference[6]. The advantage with respect of Reference[6] is that the solution has been proved explicitely under the hypothesis of Low Magnetic Reynolds and this helps in evaluating its range of validity. On the base of the stationary solution a lumped parameter model has been derived. The model is able to give information about both the electric and dynamic behaviour of the device. Informations about the performances of the device have been provided and a parametric study has been conducted to point out the influences of the electric conductivity of the working fluid on the performances of the device.

NOTATION

σ	Electric conductivity $[S/m]$
ρ	Density $[Kg/m^3]$
ν	Kinematic Viscosity $[m^2/s]$
μ_m	Magnetic Permeability $[H/m]$
U	Velocity $[m/s]$
B	Magnetic Field $[T]$
E	Electric Field $[V/m]$
J	Electric Current Density $[A/m^2]$
I	Electric Current $[A]$
ϕ	Electric Potential $[V]$
Γ	Angular Momentum $[Nms]$
ω	Angular Velocity $[rad/s]$
K_{vis}	Viscous Shear Coefficient $[Nms]$
K_I	Torque Coefficient $[Nm/A]$
K_{BEMF}	Back Electromotive force Coefficient $[Vs]$
R_{eq}	Equivalent Electric Resistance $[\Omega]$
r, z, θ	Cylindrical Reference Frame

REFERENCES

[1] N. A. Nobari and A. K. Misra, "Satellite Attitude Stabilization Using Four Fluid Rings," *AIAA Guidance, Navigation, and Control Conference, Toronto, Canada*, 2010.

[2] K. D. Kumar, "Satellite Attitude Stabilization Using Fluid Rings," *Acta Mechanica Online*, Vol. 208, No. 12, 2009, pp. 335–348.

[3] C. Casteras, Y. Lefevre, and D. Harribey, "Magnetohydrodynamic inertial actuator," 2013. WO Patent App. PCT/EP2013/053,101.

[4] D. R. Laughlin, H. R. Sebesta, and D. E. Ckelkamp-Baker, "A Dual Function Magnetohydrodynamic (MHD) Device for Angular Motion Measurement and Control," *Advances in the Astronautical Sciences*, Vol. 111, 2002, pp. 335–348.

[5] P. Davidson, *An Introduction to Magnetohydrodynamics*. Cambridge University Press, 1st ed., 2001.

[6] D. C. Moynihan and S. G. Bankoff, "Magnetohydrodynamic circulation of a liquid of finite conductivity in an annulus," *Appl. sci. Res.*, Vol. 12, No. B, 1964, pp. 165–202.

[7] J. A. Shercliff, "Steady motion of conducting fluids in pipes under transverse magnetic fields," *Mathematical Proceedings of the Cambridge Philosophical Society*, Vol. 49, No. 01, 1953, p. 136 144.